

Structural, Optical, Electrical and Biological Evaluation of a 3,5-Dimethylpyrazole Benzilic Acid Crystal

Siva Govindasamy^a, Bharathikannan Rajakannu^{a*}, Mohanbabu Bharathi^b, Tamiloli Devendhiran^c and Mei-Ching Lin^c

^aDepartment of Physics, Sri Ramakrishna Mission Vidyalaya College of Arts and Science, Tamil Nadu, India

^bDepartment of Physics, Sri Shakthi Institute of Engineering and Technology, Tamil Nadu, India

^cDepartment of Applied Chemistry, Chaoyang University of Technology, Taichung, Taiwan, R.O.C.

Abstract: A single crystal of charge-transfer 3,5-dimethylpyrazole benzilic acid (DMPBA) was grown at room temperature by using a slow evaporation solution growth technique. The grown crystal belonged to the monoclinic system with the space group of $P2_1/n$. Different spectroscopic and analytical techniques were used for analyzing the structure and properties of the grown crystal, such as Fourier transform infra-red, UV-Vis, ^1H and ^{13}C nuclear magnetic resonance. The mechanical strength of the crystal has been studied by using a Vickers' micro-hardness test. The stiffness constant and yield strength of the crystal were also calculated from the micro-hardness test and Z-scan studies. The thermal stability of the crystal was studied by using thermo-gravimetric and differential thermal analysis and was found to be stable up to 187.6°C . In addition, the newly synthesized DMPBA compound was tested for deoxyribonucleic acid (DNA) binding, and *in vitro*-antimicrobial activity against various bacterial and fungal species. Also, the compound showed the moderate capacity of scavenging with 2,2-diphenyl-1-picrylhydrazyl (DPPH).

Keywords: 3,5-dimethylpyrazole benzilic acid crystal; photophysical properties; Z-scan; biological activity.

1. Introduction

In recent years, organic nonlinear optical (NLO) materials are extremely attracted by researchers thanks to their potential applications like photonics, opto-electronics, optical laser induced technologies and biological studies [1-8]. Further, the NLO crystalline materials second and third order effects of properties chiefly influenced by the orientation of molecules within the lattice in centro and non-centro symmetric arrangement and magnitude of high molecular hyperpolarizability β [9-11]. Many ways are projected to attain noncentrosymmetric space lattice like contain heteroatoms, introducing chiral center and using non-covalent interactions [12, 13]. The electron rich donor (D) mix with electron deficient acceptor (A) to create delocalized electronic structure of π -conjugated D-A systems, that provides variety of enticing prospects with high response NLO material [14, 15]. The benzilic acid moiety combined with azole systems to create D-A structured molecule with sensible NLO properties that encourage effective intra molecular charge-transfer (ICT) properties. The effective ICT properties are widely used to deoxyribonucleic acid binding and antimicrobial activity with charge transfer complexes.

*Corresponding author; e-mail: rbkrys@gmail.com

doi:10.6703/IJASE.202005_17(2).135

©2020 Chaoyang University of Technology, ISSN 1727-2394

Received 24 April 2019

Revised 24 February 2020

Accepted 25 March 2020

The 3,5-dinitrobenzoic acid is one in all the well-known π -conjugated acceptor and it pronto to just accept an electron from donor materials like *p*-phenylenediamine, *p*-toluidine, 2,6-diaminopyridine, quinuclidine and norfloxacin. In recent reports, *p*-phenyldiamine with picric acid and 3,5-dinitrobenzoic acid ICT properties were investigated in both states (solid and liquid) [16-18]. The 3,5-dimethylpyrazole compound contains nitrogen strength are often augmented by the presence of two methyl groups in third and fifth position, respectively [19, 20]. One amongst the expected approaches may be a proton transfer between two separate organic molecules as an example acidic to basic (or) cation to anion mixtures to boost their asymmetric nature of crystal [21]. Murugesan et al. [5] stated D-A type co-crystal of 2,6-diaminopyridine and 4-nitrophenylacetic acid for biological applications. The D-A kind crystal confirmed effective charge transfer properties with appropriate antimicrobial activity. Saravanabhavan et al. [22] suggested the adduct crystal of carbazole picrate (CP) utilized DNA binding studies. The adduct crystal CP binds with DNA through intercalation with intrinsic binding constant (K_b) value of $2.9 \times 10^4 \text{ M}^{-1}$ [23]. In accordance, to above reviews, a systematic technique was performed to achieve 3,5-dimethylpyrazole based new organic NLO materials which resulted in the invention of 3,5-dimethylpyrazole-benzilic acid form pyrazole family. The grown crystals had been subjected to numerous characterization techniques which includes crystal structure has been decided through single crystal XRD, FT-IR, NMR analysis, UV-Vis, PL and Z-scan studies and the outcomes are mentioned in detail. The DMPBA has been characterized through elemental analysis. DMPBA charge transfer complex was screened for its antibacterial and antifungal activity against diverse strains and antioxidant study additionally characterized. Inside the present investigation, it's far aimed to set off huge NLO response by way of occurring of charge transfer among 3,5-dimethylpyrazole benzilic acid. The work reports the synthesis, spectral, structural, thermal analysis and biological evaluation of a new 3,5-dimethylpyrazole benzilic acid crystal. The Z-test study has found out that the title compound exhibits third order nonlinear effect.

2. Experimental Methods

2.1 Synthesis and Growth of Single Crystal

Equimolar ratio of 3,5-dimethylpyrrole and benzilic acid had been prepared separately in methanol and henceforth mixed collectively. The resulting solution was stirred well for approximately half an hour when a precipitate compound was obtained. The product was filtered off and repeatedly recrystallized from methanol to enhance the quality of the product. The solution was then filtered through a quantitative Whatman@ grade41 filter paper to dispose of the suspended impurities. The filtrate was kept aside unperturbed in a dust-free room for the growth of single crystals. Properly-defined crystals have been accrued on the end of fifteenth day.

2.2 Characterization Techniques

The prepared samples had been characterized and investigated for structural, optical, morphological, electric and biological studies. Elemental analysis (C, H and N) was executed on a Perkin Elmer 240C elemental analyzer at university of Hyderabad, Hyderabad, India. The electronic absorption spectrum was measured in methanol using SHIMADZU 1601 UV-Vis spectrophotometer within the range of 200-800 nm with a purpose to verify the functional groups, the crystal was subjected to FT-IR spectral evaluation with the aid of Perkin Elmer FT-

IR 8000 spectrophotometer in the range of 4000-400 cm^{-1} using the KBr pellet technique. ^1H and ^{13}C NMR spectra have been recorded using Bruker AV III 500 MHz spectrometer device using TMS as an internal standard. Thermal properties of DMPBA single crystal have been studied by thermogravimetric analysis (TGA) and differential thermal analysis (DTA), which were performed between 25°C and 600°C in nitrogen environment at a heating rate of 10°C min^{-1} using NETZSCH STA 409 C/CD TG/DTA instrument. Dielectric studies had been carried out within the frequency range from 50 Hz to 200 KHz at different temperatures using a HIOKI LCR 3532-50 LCR meter. Micro hardness studies for the grown crystals were carried out using a LEITZ WETZLAR Vickers micro hardness pyramidal indenter attached to an incident light microscope by means of various the load from 10 to 300 g. The single beam Z-scan experimental technique was used to determine the value and higher order nonlinearity of the grown crystal. The nonlinear refractive index (n_2) and nonlinear absorption coefficient (β) had been investigated. An antioxidant and antimicrobial study were done at the Kovai medical Centre and hospital Pharmacy College, Coimbatore, Tamil Nadu, India.

2.3 Single Crystal X-ray Diffraction Studies

The single crystal X-ray diffraction information of DMPBA crystal was done on a Bruker AXS KAPPA APEX2 CCD diffractometer geared up with a best centered sealed tube at room temperature. The information collection of DMPBA and the determination of unit cell parameters was acquired via using a graphite-mono chromate $\text{Mo } \alpha$ ($\lambda = 0.71073 \text{ \AA}$) radiation by φ and ω scans by the use of SHELXS-97, the structure of the compound became solved with the aid of direct techniques [24]. Wherein the position of all non-hydrogen atom became discovered, and was refined through full-matrix least squares on F2 (SHELXL-97) [25]. All non-hydrogen atoms were refined anisotropically, while the hydrogen atoms were placed in the calculated positions and delicate as riding atoms.

2.4 Biological Evaluation

2.4.1 DNA Binding - Titration Experiments

The binding affinities of all the compounds with CT-DNA have been done in doubly distilled water with Tris(hydroxymethyl)-aminomethane (Tris, 5 mmol) and sodium chloride (50 mmol) and the pH of the solution is adjusted to 7.2 with hydrochloric acid. A solution of CT-DNA in the buffer gave a ratio of UV absorbance of approximately 1.8-1.9 at 260 nm and 280 nm which indicated that the DNA was sufficiently freed from protein. The DNA concentration according to nucleotide was determined via absorption spectroscopy using the molar extinction coefficient value of 6600 $\text{dm}^3 \text{ mol}^{-1} \text{ cm}^{-1}$ at 260 nm. The compounds have been dissolved in a solvent mixture, comprising of 5 % DMSO and 95 % Tris-HCl buffer for all the experiments. Stock solutions were stored at 4°C and used within 4 days. Absorption titration experiments were carried out with fixed concentration of the compounds (25 μM) with various concentration of DNA (0-60 μM). At the same time as measuring the absorption spectrum, an equal quantity of DNA was introduced to the all test solutions and the reference technique to eliminate the absorbance of DNA itself [22].

2.4.2 Antibacterial Activity

The antibacterial activity of newly synthesized compound was tested *in vitro* against Gram-positive bacteria *Staphylococcus aureus* and *Bacillus subtilis* and two Gram-negative bacteria *Pseudomonas aeruginosa* and *Klebsiella pneumoniae*. DMSO solvent was used and set up as control. The discs measuring 5 mm in diameter had been prepared from Whatman@ No.1 filter paper and sterilized by way of dry heat at 140°C for 1 h. The sterile discs had been soaked previously in concentrated test solution and have been positioned in nutrient agar medium. The Petri plates have been invested and kept in an incubator for 24 h at 37°C and growth was monitored visually. The screening was finished at 100 µg/mL concentration of test compound with antibiotic disc. Ciprofloxacin (30 mg/disc) was used as control. Logarithmic serially -fold diluted amount of test compound and controls was inoculated within the range 10^{-4} - 10^{-5} cfu/mL. To attain the diameter of sector, 0.1 mL quantity was taken every and spread on agar plates. The number of colony forming units (cfu) was counted after 24 h of incubation at 35°C. After incubation the zone of inhibition was measured and expressed as mm in diameter [26, 27].

2.4.3 Antifungal Activity

The newly synthesized compound was additionally screened for its antifungal property against *Aspergillus niger*, *Aspergillus fumigatus* and *Candida albicans* in DMSO solvent via the usage of preferred agar disc diffusion method. The synthesized compound was dissolved in DMSO solvent and media with DMSO was set up as control. All cultures were routinely maintained on Sabouraud Dextrose Agar (SDA) and incubated at 28°C. Spore formation of *filamentous fungi* was formed from seven days old culture on sterile normal solution, which was diluted to about 10^5 cfu/mL. The culture was centrifuged at 1000 rpm, pellets have been resuspended and diluted in sterile normal Saline solution (NSS) to attain a viable count 10^5 cfu/mL. With the help of spreader, 0.1 mL volume of approximately diluted fungal culture suspension was taken and spread on agar plates. The fungal activity of compound was compared with Clotrimazole (30 g/disc) which is used as standard drug. The cultures were incubated for 48 h at 37°C and the growth was monitored. Antifungal activity was determined by means of measuring the diameters of the zone (mm) in triplicate sets.

2.4.4 Antioxidant Activity

The 2,2-diphenyl-2-picryl-hydrazyl (DPPH) radical scavenging activity of the compound was measured according to the method of Elizabeth and Rao [28]. The DPPH radical is a stable free radical having a λ_{\max} at 517 nm. A fixed concentration of the experimental compound (100 µL) was added to a solution of DPPH in methanol (0.3 mM, 1 mL) and the final volume was made up to 4 mL with double distilled water. DPPH solution with methanol was used as a positive control and methanol alone acted as a blank. The solution was incubated at 37°C for 30 min in dark. The decrease in absorbance of DPPH was measured at 517 nm. The scavenging activity for hydroxyl radicals recommended by Yu et al., with major changes [29]. Reaction mixture contained 0.6 mL of 1.0 mM deoxyribose, 0.4 mL of 0.2 mM, phenyl hydrazine and 0.6 mL of 10 mM phosphate buffer (pH 7.4). It was incubated for 1 h at room temperature. Then, 1 mL of 2-8% TCA, 1 mL of 1% TBA and 0.4 mL of extract at various concentrations were added and kept in water bath for 20 min. The absorbance of the mixture at 532 nm was measured with a spectrophotometer. The hydroxyl radical-scavenging activity was calculated. For the above assays, the tests were run in triplicate by varying the concentration. The percentage inhibition of absorbance was calculated and plotted as a function of the concentration of standard and sample to determine the antioxidant concentration. The percentage activity was calculated by using the formula % activity = $[(A_o - A_c)/A_o] \times 100$,

where A_o and A_c represent the absorbance in the absence and presence of the test compound. The 50% activity (IC_{50}) is calculated from the result of percentage activity. Ascorbic acid was used as a standard for all the above assays.

3. Result and Discussion

3.1 Elemental Analysis

The chemical composition of the essential elements (CHN) present in the synthesized compound was verified through elemental analysis. The micro analysis results showed that the compound DMPBA contained C: 70.12% (70.35%), H: 5.09% (6.21%) and N: 7.58% (8.64%). The study data specified that the experimentally determined values were in well agreement with theoretical values (within the bracket). The results showed that the DMPBA was free from impurities and confirmed the formation of the compound in the stoichiometric proportion.

3.2 Electronic Absorption Spectral Analysis

The electronic absorption spectrum for the grown crystal in methanol was recorded in the range of 200-800 nm and is shown in Figure 1a. This spectrum gives two peaks, one at 225 nm and one at 260 nm. The peaks at 225 nm and 260 nm are corresponding to π - π^* and n - π^* transitions of DMPBA, respectively. The observed low UV cut-off wavelength of 260 nm indicated that this material is a potential candidate for generating blue-violet light using a diode laser. The UV cut-off below 300 nm is sufficiently low for a SHG laser radiation at 1064 nm or other applications in the blue region [30]. There is no absorption peak observed between 280 and 800 nm. This transparent nature of the crystal shows that DMPBA can be exploited for several NLO applications [31].

3.3 Photoluminescence (PL) Studies

Currently organic crystalline materials have high potential applications in fabricating light emitting devices (LEDs). Based on the need of organic LEDs, the luminescent behaviour of the grown single crystal was analyzed by recording the PL spectrum. PL study is a significant method to evaluate the optical properties of the grown organic crystal for possible photonic applications. Besides, the PL study is also useful for examining organic compounds in the field of chemical research, biomedical and biology [32]. The PL property of an organic complex basically depends on the presence of localized π -electron systems in the molecules. Nevertheless, the intensity of the incident beam and the density of photons also alter the PL signal from a crystalline compound. Figure 1b shows the PL emission spectrum of the DMPBA crystal. The maximum emission wavelength is observed at 330 nm excited at 230 nm and this peak corresponds to violet wavelength emission. The violet emission was due to the donation of protons to the amino group from the carboxylic acid in the molecule.

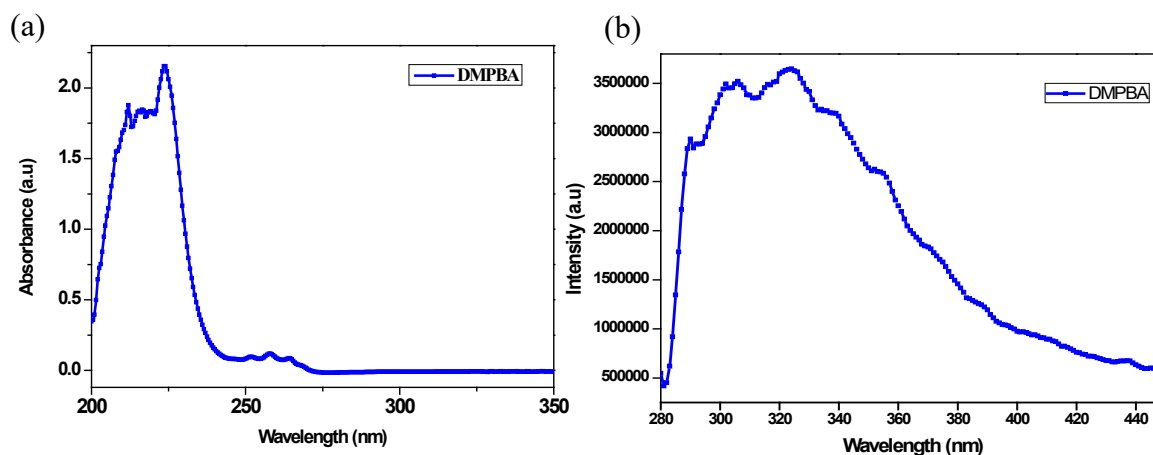


Figure 1. (a) UV-Visible absorption and (b) fluorescence emission spectra of DMPBA.

3.4 Vibrational Analysis

The well assignment of the bands, observed in the vibrational spectra is an indispensable step for solving the structural problems of any molecule. The IR spectrum of DMPBA in the region 4000–400 cm^{-1} is shown graphically in Figure 2 and the corresponding vibrational wavenumbers are given in Table 1. The details of the various vibrations and their assignments are discussed in the subsequent sections. The broad absorption band appearing at 3318 cm^{-1} is due to O-H asymmetric stretching vibration of the benzoic acid moiety. The sharp absorption band at 3100 cm^{-1} is due to the asymmetric aromatic C-H stretching vibration. The aliphatic C-H stretching vibration is observed at 2900 cm^{-1} . The C=N stretching vibration appears at 2335 cm^{-1} . The band at 1692 cm^{-1} is due to the C=C stretching vibration. The COO-asymmetric stretching vibration and the COO-symmetric stretching vibration are observed at 1631 cm^{-1} and 1352 cm^{-1} respectively. The O-H out of plane bending is observed at 1183 cm^{-1} . The C-H in plane bending vibration and the C-H out of plane bending are observed at 1134 cm^{-1} and 733 cm^{-1} respectively. The C-N stretching vibration appears at 611 cm^{-1} .

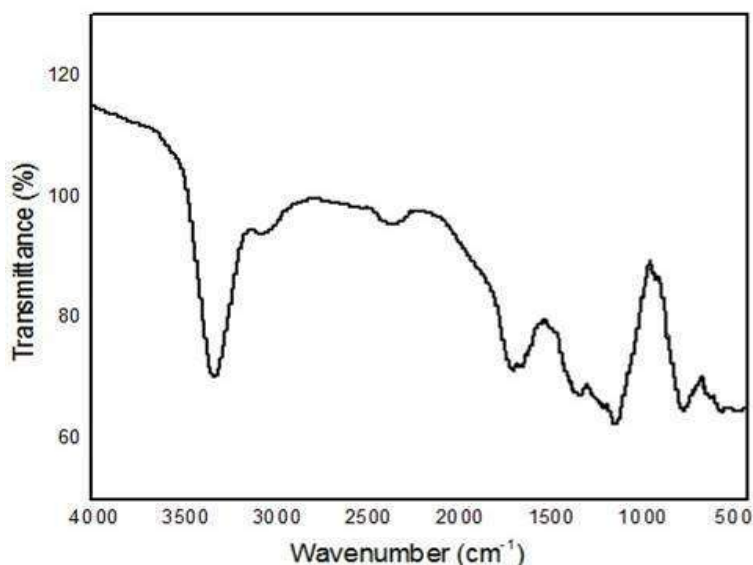


Figure 2. FT-IR spectrum of DMPBA.

Table 1. FT-IR spectral band assignments of DMPBA crystal.

Infrared frequencies (cm ⁻¹)	Assignment
3318	O-H stretching vibration
3100	C-H aromatic stretching vibration
2700	C-H aliphatic stretching vibration
2335	C=N stretching vibration
1692	C=C stretching vibration
1631	COO ⁻ asymmetric stretching vibration
1352	COO ⁻ symmetric stretching vibration
1183	O-H out of plane bending
1134	C-H in plane bending
733	C-H out of plane bending
611	C-N stretching vibration

3.5 NMR Spectral Analysis

Nuclear magnetic resonance (NMR) is a versatile technique employed to identify the molecular structure. The ¹H NMR and ¹³C NMR spectra of DMPBA were recorded using deuterated methanol as solvent and TMS as internal standard reference. The recorded ¹H and ¹³C NMR spectra are shown in Figure 3, respectively and the chemical shifts are tabulated in Table 2. In the ¹H NMR spectrum the appearance of six distinct proton signals confirms the formation of the salt crystal. The singlet at δ 7.4 ppm is due to the C2 and C6 aromatic proton of the same kind in benzilic acid moiety. The triplet peak centered at δ 7.25 ppm is assigned to the C4 aromatic proton of the benzilic acid moiety. The doublet of centered at δ 7.1 ppm owes to the C3 and C5 aromatic proton of the benzilic acid moiety. The methine proton of 3,5-dimethyl pyrazole moiety appears at δ 4.62 ppm. The two OH protons of benzilic acid moiety appear as a small hump at δ 2.4 ppm. The intense singlet signal observed at δ 2.0 ppm represents the protons due to two identical methyl protons of the 3,5-dimethyl pyrazole moiety. The appearance of ten distinct carbon signals in the spectrum explicitly confirms the molecular structure of the complex salt crystal. The carbon signal at δ 206 ppm owes to the highly deshielded carboxyl carbon atoms of the benzilic acid moiety. The carbon signal at δ 174.79 ppm is attributed to the C1 carbon of the benzilic acid moiety. The weak carbon signal at δ 143.74 ppm is attributed to the C3 carbon of the benzilic acid moiety. The carbon signal at δ 142.79 ppm is due to the C3 and C5 carbon of 3,5-dimethylpyrazole moiety. The C2 carbon of the benzilic acid moiety appears at δ 127.71 ppm. The signal at 127.14 ppm owes to the C4 carbon of the benzilic acid moiety. The C4 carbon of the 3,5-dimethylpyrazole moiety appears at δ 103.27 ppm. The carbon signal observed at δ 80 ppm is assigned to methane carbon of the benzilic acid moiety. The methine carbon of 3,5-dimethylpyrazole moiety stands responsible for the carbon signal at δ 30 ppm. The methyl carbon signal of 3,5-dimethylpyrazole moiety appears at δ 11.94 ppm. Thus, the molecular structure of salt crystal stands confirmed from the ¹H and ¹³C NMR spectral data.

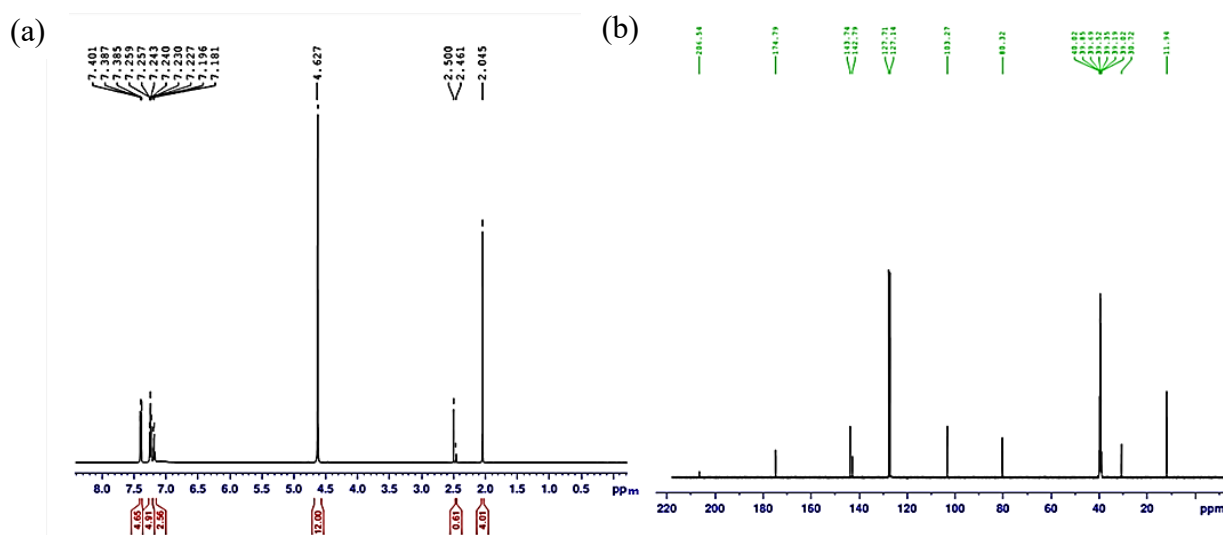


Figure 3. (a) ^1H and (b) ^{13}C NMR spectra of DMPBA.

Table 2. ^1H and ^{13}C NMR chemical shift values of DMPBA crystal.

Chemical shift value (ppm)	Assignment
The ^1H NMR spectral data	
7.4	C2 and C6 aromatic proton of same kind in benzoic acid moiety.
7.25	C4 aromatic proton of benzoic acid moiety.
7.1	C3 and C5 aromatic proton of same kind in benzoic acid moiety.
4.62	CH of 3,5 dimethyl pyrazole moiety
2.4	OH proton of benzoic acid moiety.
2.0	Methyl proton of 3,5 dimethyl pyrazole moiety
^{13}C NMR spectral data	
206	Carbonyl carbon of benzoic acid moiety
174.79	C1 carbon of the benzoic acid moiety.
143.74	C3 carbon of the benzoic acid moiety
142.79	C3 and C5 carbon of 3,5 dimethylpyrazole moiety
127.71	C2 carbon of the benzoic acid moiety.
127.14	C4 carbon of the benzoic acid moiety.
103.27	C4 carbon of the 3,5dimethylpyrazole moiety.
80	CH of the benzoic acid moiety.
30	C3 Methyl carbon of 3,5 dimethylpyrazole moiety
11.94	C5 Methyl carbon of 3,5 dimethylpyrazole moiety

3.6 TG/ DTA Analysis

The thermal stability of DMPBA was identified by the Thermo Gravimetric (TG) and Differential Thermal analysis (DTA) and the recorded thermogram is shown in Figure 4. The TG curve of the material reveals two stage decomposition patterns. The DTA reveals the same changes shown by the TGA. In the DTA curve there is a sharp endothermic peak at 132.5°C indicating the melting point of the material. The sharpness of the endothermic peak shows a good degree of crystallinity and purity of the material [33]. From the TG curve it has been understood that the material decomposed immediately after melting and the first stage decomposition continued up to 158°C with elimination of about 93.8% of the material as gaseous products. The bulk decomposition of the compound took place before 284°C. The DTA curve shows the second endothermic peak at 245°C. This event represents the evaporation of the volatile materials.

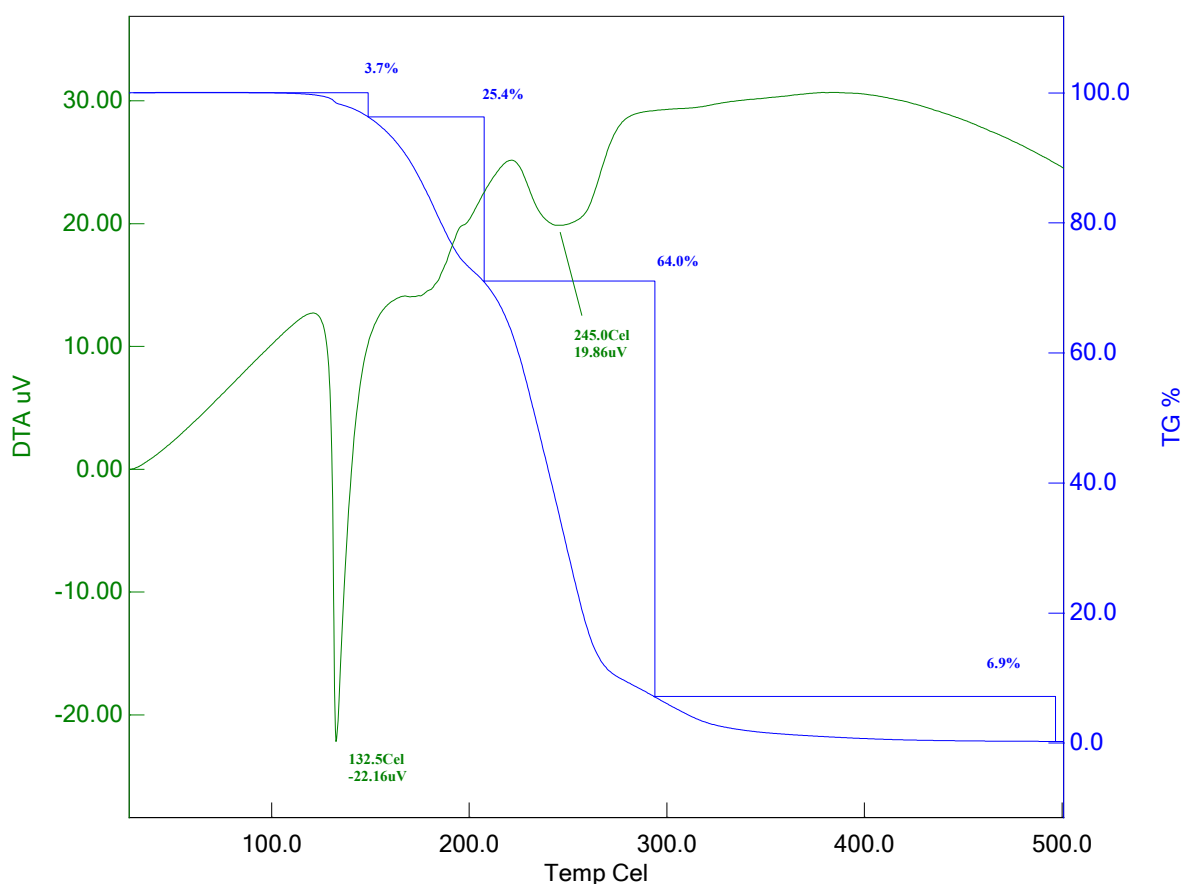


Figure 4. TGA and DTA curve of DMPBA.

3.7 Single Crystal X-ray Diffraction Analysis

The grown DMPBA single crystal was subjected to single crystal X-ray diffraction analysis. The obtained crystallographic data are given in the Table 3. The single crystal structure determination of DMPBA has been carried out at room temperature using a Brukeraxs (Kappa apex2) diffractometer at 293 K using Mo K α radiation ($\lambda = 0.71073 \text{ \AA}$). The unit cell parameters were obtained by using many high angle reflections. The structure was solved by using SHELXS 97 (Sheldrick 1997) and refined by full-matrix least-squares refinement method using SHELXL 97 (Sheldrick 1997) program. The intensity data were collected for h from -8 to 8, for k from -23 to 23 and for l from -20 to 20. From the single crystal X-ray diffraction data, it is confirmed that the grown crystal belongs to the monoclinic system with centrosymmetric space group $P2_1/n$. The lattice parameters value was $a = 9.2507 (18) \text{ \AA}$, $b = 9.4690 (19) \text{ \AA}$, $c = 19.446 (4) \text{ \AA}$, $\alpha = 90^\circ$, $\beta = 91^\circ$, $\gamma = 90^\circ$ and the unit cell volume was 1702.34 \AA^3 . The ORTEP of the molecule with displacement ellipsoids at 40% probability level are given in Figure 5. The stacking shows a strong interaction existing between 3,5-dimethylpyrazole and benzoic acid moieties. The selected bond lengths and bond angles are analysed to understand the structural property. In the benzoic acid $C_{12}-O_1$ the bond distance was 1.4212 \AA and the bond lengths $C_{12}-C_{13}$, $C_{12}-C_{19}$ were 1.5567 \AA and 1.5237 \AA which indicate that the bond length of the $C_{12}-O_1$, $C_{12}-C_{13}$, $C_{12}-C_{19}$ are different from the standard aromatic C-C, C-O bond lengths. These differences are attributed to the $C_{12}-C_{13}$, $C_{12}-C_{19}$, $C_{12}-C_{11}$ which are deviated from the plane of the ring. Whereas, the C_3-N_1 bond length was 1.471 \AA which shows that the C_1-N_2 bond was lying in the plane of the ring.

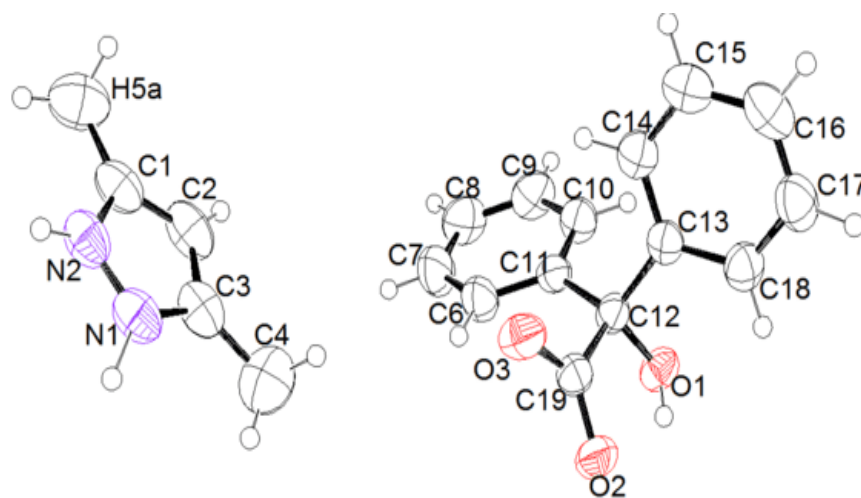


Figure 5. ORTEP diagram of DMPBA.

Table 3. Crystal data and structure refinements of DMPBA crystal.

Identification code	shelxl
Empirical formula	C ₁₉ H ₂₀ N ₂ O ₃
Formula weight	324.37
Temperature	273 K
Wavelength	0.71073 Å
Crystal system, space group	monoclinic, <i>P2₁/n</i>
Unit cell dimensions	a = 9.2507(18) Å alpha = 90.000 deg.
	b = 9.4690(19) Å beta = 91.995(3) deg.
	c = 19.446(4) Å gamma = 90.000 deg.
Volume	1702.34 Å ³
Z, Calculated density	34, 1.427 Mg/m ³
Absorption coefficient	0.128 mm ⁻¹
F(000)	748
Crystal size	0.24 x 0.19 x 0.16 mm ³
Theta range for data collection	2.10 to 26.04 deg.
Limiting indices	-11 ≤ h ≤ 11, -11 ≤ k ≤ 11, -23 ≤ l ≤ 23
Reflections collected / unique	17103 / 3359 [R(int) = 0.0421]
Completeness to theta	26.04 99 %
Absorption correction	Semi-empirical from equivalents
Max. and min. transmission	0.960 and 0.972
Refinement method	Full-matrix least-squares on F ²
Data / restraints / parameters	3359 / 0 / 275
Goodness-of-fit on F ²	1.060
Final R indices [I > 2σ(I)]	R1 = 0.0535, wR ² = 0.1364
R indices (all data)	R1 = 0.0688, wR ² = 0.1464
Extinction coefficient	0.0015(8)

3.8 Measurement of Microhardness

Microhardness studies were carried out on the grown crystal to study the mechanical properties of the grown crystals. The static indentations were made at the room temperature with a constant indentation time of 15 seconds for all indentations. The indentation marks were made on the surfaces by the variation of the load from 25 to 300 g. The Vickers micro-hardness number Hv of the crystal was calculated using the following relation,

$$H_v = 1.8544 P/d^2 \text{ Pascal} \quad (1)$$

Where, P is the applied load and d the average diagonal length of the indented impressions in meter. Figure 6a shows the Vickers micro-hardness as a function of the applied test loads. It is evident from the plot that the micro-hardness values of the grown crystal with an increasing load agrees with the normal indentation size effect. The Meyer's index number was calculated from Meyer's law, which relates the load and indentation diagonal length and is given by $P = kd^n$, where k is the material constant and n is Meyer's index.

The plot between log P and log d is shown in Figure 6b. The slope of the straight-line plot gives the value of n and is found to be 2.123. Hv should increase with an increase of P if $n > 2$ and decrease if $n < 2$. When $n = 2$, the hardness is independent of the load applied and is given by Kick's law [34]. Then, the value agrees well with the experiment. According to Onitsch and Hannemann it should lie between 1 and 1.6 for harder materials and for softer materials n should be above 1.6 [35, 36]. Thus, crystal belongs to the soft material category ($n = 2.123$). The stiffness constant gives details about the nature of the bonding between the neighbouring atoms. The stiffness constant is the property of the material by which it can absorb the maximum energy before fracture occurs. The stiffness constant is calculated from Wooster's empirical relation, $H_v^{7/4}$ [37]. The variation of the stiffness constant with various loads is shown in Figure 6c. From the hardness values, the yield strength (σ_v) can be calculated. The yield strength is defined as the stress at which the material begins to deform plastically. The value of the yield strength depends on Meyer's index number n. For $n > 2$, σ_v can be calculated using the expression. It is seen from Figure 6d, that the yield strength also increased as the load was increased.

$$\sigma_v = \frac{3-n}{2.9} \left(\frac{12.5(n-2)}{3-n} \right)^{n-2} H_v \tag{2}$$

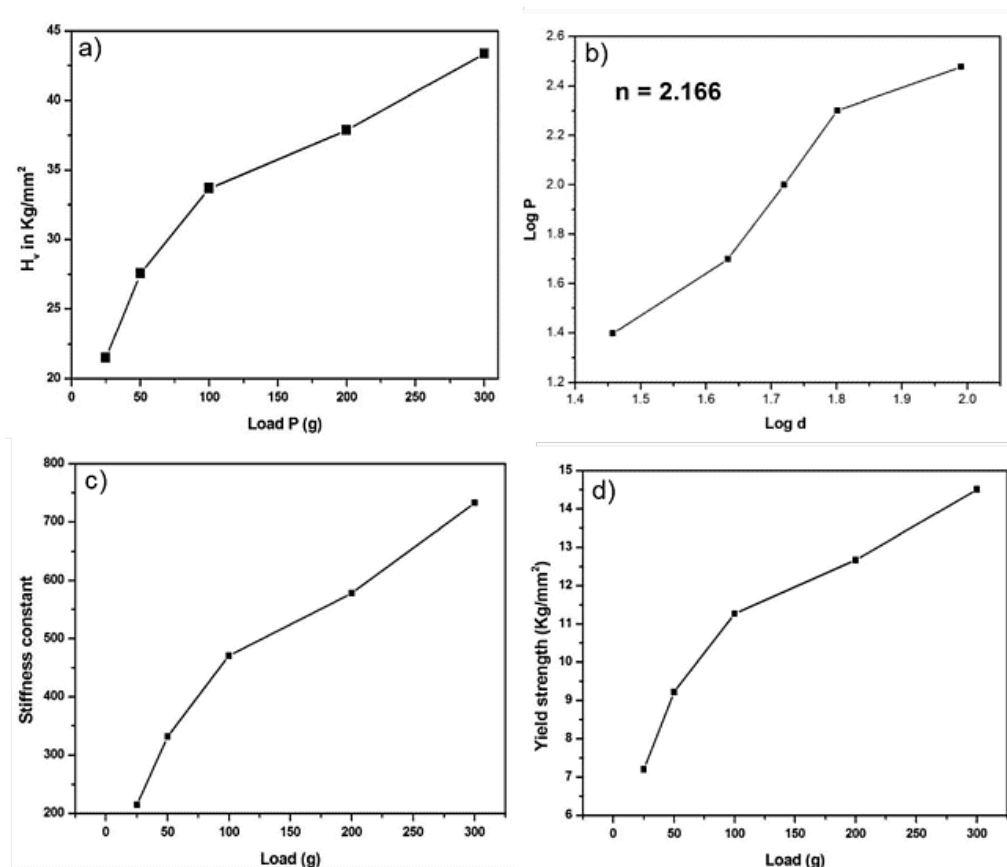


Figure 6. (a) The Vickers micro hardness profile as a function of the applied test loads. (b) The plot between log p and log d. (c) The variation of stiffness constant. (d) The variation of yield strength of DMPBA.

3.9 Dielectric Study

The study of dielectric property plays an important role to understand the electrical properties that are directly interconnected with the electro-optic properties of crystals. They provide valuable information about the structural, defect and polarization behaviour of the crystals. Currently, the microelectronics industry requires low dielectric constant materials for preparation of interlayer dielectrics to decrease RCT delay, lower power consumption and reduce crosstalk between nearby interconnects. Dielectric measurement is one of the techniques to analysis the electrical response of solids. The study of the dielectric properties of solids gives the information about the electric field distribution within the solid. The frequency dependence of these properties gives a great insight into the material's applications. The different polarization mechanisms in a grown crystal is understood from the study of the dielectric constant as a function of frequency and temperature. The capacitance of the crystal was measured for the frequency range of 50Hz-200 kHz at various temperatures of 25°C, 35°C and 45°C. The plot of dielectric constant (ϵ_r) and frequencies is shown in Figure 7a. The dielectric constant of the crystal was calculated by using the relation $\epsilon_r = C_{\text{crys}}d/\epsilon_0A$, where C_{crys} is the capacitance of the crystal, d is the thickness of the sample, ϵ_0 is the permittivity of free space and A is the area of the sample used. The dielectric constant has higher values in the lower frequency region and then it decreased with an increasing frequency. The contribution of space charge, orientation, electronic, and ionic polarizations reduces gradually at higher frequencies. This is the reason for the low value of dielectric constant at higher frequencies. The defects have no long enough time to rearrange in response to the applied voltage at higher frequency. Hence the capacitance of the sample decreased with increasing frequency. The function of dielectric loss with log frequency is shown in Figure 7b. The characteristic of low dielectric loss at high frequencies for a given sample suggested that the sample possesses an enhanced optical quality with lesser defects. Hence, the grown crystals may be useful in fabrication of nonlinear optical devices [38, 39].

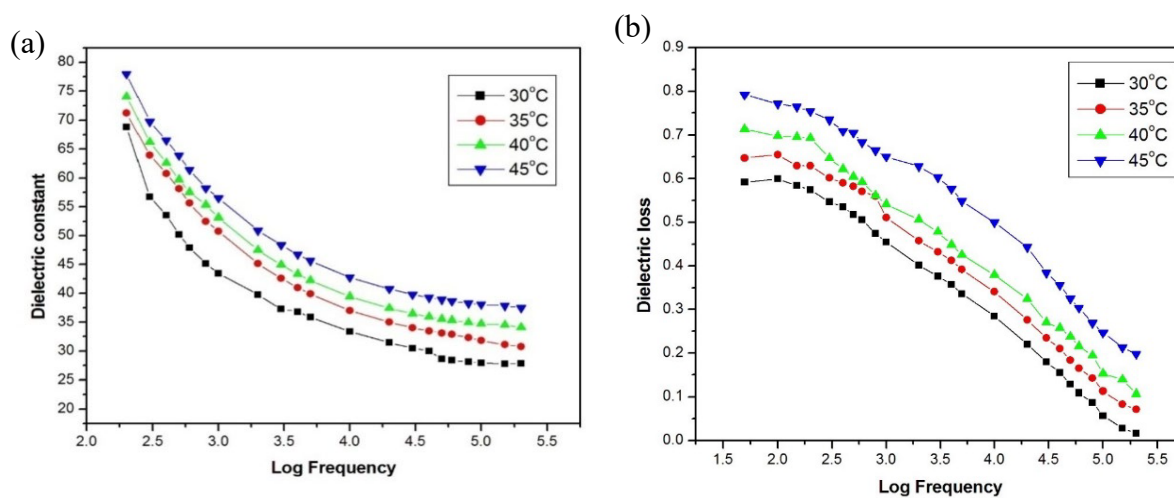


Figure 7. (a) The plot of dielectric constant and log frequencies and (b) The function of dielectric loss with log frequency of DMPBA.

3.10 Z-Scan Analysis

The Z-scan is a well-known experimental technique to measure the intensity dependent third order nonlinear susceptibility of the materials [40, 41]. The open and closed aperture Z-scan configurations are used to investigate the nonlinear absorption coefficient β and nonlinear refractive index n_2 , respectively. Figure 8a and Figure 8b show the normalized transmittance (T) with closed aperture and open aperture, respectively as a function of the distance z along the lens axis in the far field. The nonlinear refractive index (n_2) of the crystal was calculated using the standard relations given below

$$\Delta\phi_0 = \frac{\Delta T_{p-v}}{0.406 (1-s)^{0.25}} \quad (3)$$

Where, $\Delta\phi_0$ is nonlinear phase shift, ΔT_{p-v} is the difference between the normalized peak and valley transmittance and S is the linear transmittance of the aperture. The nonlinear refractive index (n_2) and nonlinear absorption coefficient (β) are given by,

$$n_2 = \frac{\Delta\phi_0}{kL_{eff}I_0} \quad \text{and} \quad \beta = \frac{2\sqrt{2}\Delta T}{I_0L_{eff}} \quad (4)$$

Where k is the wave number $k = 2\pi/\lambda$ and

$$L_{eff} = \frac{1-e^{-\alpha L}}{\alpha} \quad (5)$$

With I_0 defined as the peak intensity within the sample, where L is the thickness of the sample, and α is the linear absorption coefficient. The real and imaginary parts of the third order nonlinear susceptibility χ^3 are defined as

$$Re\chi^{(3)} = 10^{-4} \frac{(\epsilon_0 c^2 n_0^2 n_2^2)}{\pi} (esu) \quad (6)$$

$$Im\chi^{(3)} = 10^{-2} \frac{(\epsilon_0 c^2 n_0^2 \lambda \beta)}{4\pi^2} (esu) \quad (7)$$

Where ϵ_0 is the vacuum permittivity, n_0 is the linear refractive index of the sample and c is the velocity of light in vacuum. Thus, we can easily obtain the absolute value of χ^3 by the following formula

$$|\chi^{(3)}| = [(Re\chi^{(3)})^2 + (Im\chi^{(3)})^2]^{\frac{1}{2}} \quad (8)$$

As seen from the closed aperture Z scan curve the prefocal transmittance valley was followed by the post focal peak which is the positive nonlinearity [42]. The calculated value of the nonlinear refractive index n_2 is $1.092 \times 10^{-7} \text{ cm}^2/\text{W}$. The value of nonlinear absorption coefficient β estimated from the open aperture Z-scan curve is $0.36 \times 10^{-2} \text{ cm/W}$. The third order susceptibility of $\alpha\text{-LiIO}_3$ is $3.63 \times 10^{-7} \text{ esu}$. The self-focusing nature of the material has a positive refractive index, which is an essential property for all optical switching devices [43].

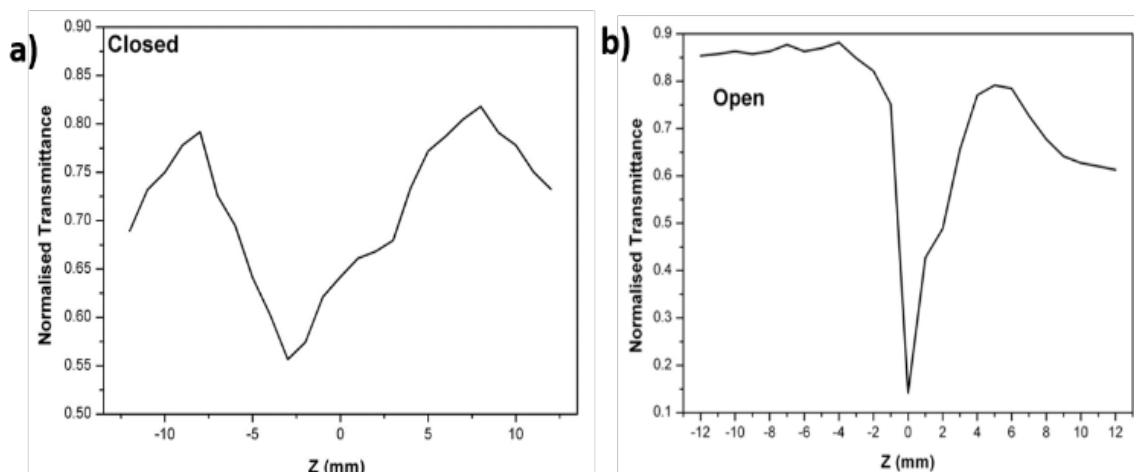


Figure 8. Z-scan spectrum of DMPBA (a) closed-aperture and (b) open-aperture.

3.11 Antimicrobial Activity Studies

3.11.1 Interaction with Calf-thymus DNA

Organic compounds can bind to double-standard DNA via non-covalent interaction that include intercalative (via π - π^* stacking interaction of the compound and DNA nucleobases), external electrostatic (as a result of coulombic forces of compounds and the phosphate groups of DNA) and groove (through Van der Waals interaction or hydrogen bonding or hydrophobic bonding along major or minor groove of DNA helix) binding of the organic compounds inside the DNA helix, along major or minor groove.

3.11.2 Study of the DNA-binding with UV Spectroscopy

Interaction of the DMPBA compound with DNA has been characterized through absorption titrations. The UV-visible spectrum of the investigated compounds in the absence as well as the presence of CT-DNA (nucleotides) was obtained in DMSO: Tris-HCl buffer (5 mmol, pH 7.2) containing 50 mmol NaCl solutions. Binding of DMPBA compound to DNA helix has been studied through the changes in intensity of absorption and shift in wavelength. The electronic absorption spectrum of the compound DMPBA measured as a function of increasing concentration of CT-DNA. Upon incremental additions of DNA to the test compounds, the absorption band of all the compounds exhibited a hypochromism of about 43% with a bathochromic shift at 4 nm. The results suggested an intimate association of the compound, DMPBA with CT-DNA and it is also likely that they bind to the DNA helix via electrostatics. After the compound electrostatics to the base pair of DNA, the π^* orbital of the electrostatics compound could couple with π orbitals of the base pairs, thus decreasing the $\pi \rightarrow \pi^*$ transition energies, resulted hypochromism [44]. In order to illustrate quantitatively the consequence, the absorption data were analyzed to evaluate the intrinsic binding constant (K_b), which can be determined from the following equation [45].

$$\text{DNA}/(\epsilon_a - \epsilon_f) = [\text{DNA}] / (\epsilon_b - \epsilon_f) + 1/K_b(\epsilon_b - \epsilon_f)$$

Where $[DNA]$ is the concentration of the DNA in the base pairs, the apparent absorption coefficients ϵ_a , ϵ_f and ϵ_b correspond to $A_{obs}/[compound]$, the extinction coefficient of the free compound and the extinction coefficient of the compound when fully bound to the DNA, respectively. From the plot of $DNA/(\epsilon_a - \epsilon_f)$ versus $[DNA]$ as shown in Figure 9, the intrinsic binding constant (K_b) was calculated by the ratio of the slope to the intercept. The magnitude of the K_b values of the Dimethyl acetylenedicarboxylate is 2.3×10^4 . Further, the observed binding constant values are comparable with the classical intercalating ethidium bromide [46].

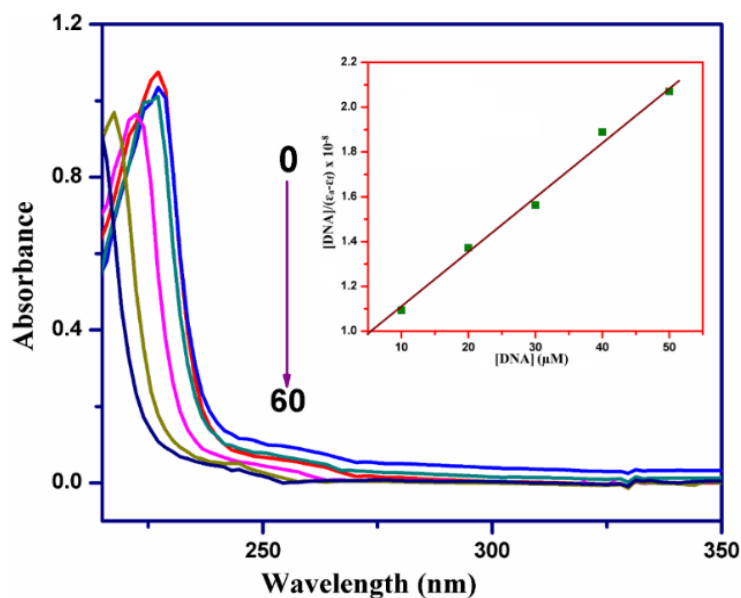


Figure 9. Electronic spectra of DMPBA in Tris-HCl buffer upon addition of CT-DNA.

3.11.3 Antibacterial Activity

DMPBA was studied for its antibacterial activities using the disc diffusion method [27, 47] against *S. aureus*, *B. subtilis*, *K. pneumoniae* and *P. aeruginosa* were prepared at a concentration of 100 $\mu\text{g/mL}$. Ciprofloxacin was used as a standard drug for the comparison of antibacterial results and the screening data are given in Table 4. DMPBA showed a very good activity against *K. pneumoniae*, which was very close to that of the standard. The synthesized compound showed significant activity against the *S. aureus* species. Also, all other bacterial species such as *P. aeruginosa* and *B. subtilis* showed moderate activity against the DMPBA compound to the standard ciprofloxacin.

Table 4. Antibacterial activity of DMPBA at the concentration of 100 $\mu\text{g/mL}$

S.NO.	organisms	Diameter of Inhibition Zone (mm)	
		DMPBA	Ciprofloxacin
1	<i>Staphylococcus aureus</i>	33	32
2	<i>Bacillus subtilis</i>	23	27
3	<i>Klebsiella pneumoniae</i>	28	27
4	<i>Pseudomonas aeruginosa</i>	24	31

3.11.4 Antifungal Activity

The antifungal activity of newly synthesized DMPBA was screened against three different fungal species viz., *C. albicans*, *A. niger* and *A. fumigatus*. Clotrimazole was used as a standard drug for comparison of antifungal activity. From the results, it is inferred that, the new DMPBA showed a good inhibitory activity against all the fungal species except *A. niger*. The results are given in Table 5.

Table 5. Antifungal activity DMPBA at the concentration 100 ug/mL.

S. No.	organisms	Diameter of Inhibition Zone (mm)	
		DMPBA	Clotrimazole
1	<i>Candida albicans</i>	15	14
2	<i>Aspergillus niger</i>	19	23
3	<i>Aspergillus fumigatus</i>	17	21

3.11.5 Antioxidant Activity

The DPPH radical has been used to test the ability of the compound as free radical and scavengers or hydrogen donors to evaluate the antioxidant activity. Hence, we carried out experiments to explore the free radical scavenging ability of 3,5-dimethylpyrazole with benzilic acid with DPPH radical and compared with those of the positive control, ascorbic acid. The compound showed a weak capacity for scavenging DPPH. The compound showed a scavenging capacity beyond 110 $\mu\text{g/mL}$. The IC_{50} values are expressed in $\mu\text{g/mL}$ of the DMPBA compound as represented in Figure 10.

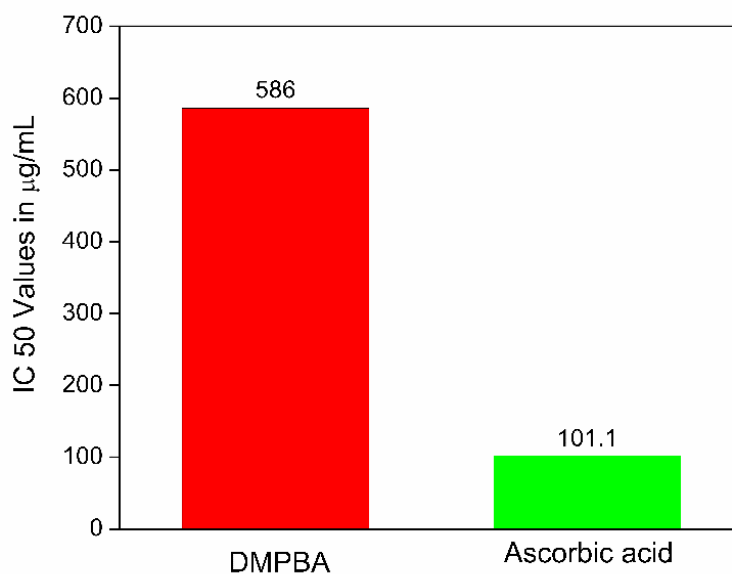


Figure 10. Antioxidant activity of DMPBA.

4. Conclusions

The organic charge transfer compound of the DMPBA was synthesized and the single crystals were grown by a slow solvent evaporation solution growth technique at ambient temperature. The unit cell parameters and the crystal structure were established by single crystal X-ray diffraction studies. The ^1H and ^{13}C NMR spectra were used to establish the molecular structure of the synthesized title crystal. The TG/DTA studies indicated that the title compound has good thermal stability. Its dielectric constant was frequency-dependent and inversely proportional to the frequency. The characteristic of low dielectric loss at high frequencies in the dielectric studies suggested that the grown crystal possessed an enhanced optical quality with lesser defects. The Z-scan experimental technique confirmed the positive refractive index and self-focusing nature of the crystal and thus suggested the third order nonlinear property of the grown crystals. The DNA binding ability of the CT complex has been observed from the absorption spectrum. The antioxidant activity exposed that the compound can assist as potential antioxidant against DPPH radicals. The antimicrobial study revealed that the compound showed activity against many microbes.

Acknowledgment

The authors thankfully acknowledge the School of Chemistry, University of Hyderabad, Hyderabad for their instrumental facilities. One of the authors G. Siva thanks the UGC Networking Centre, School of Chemistry, University of Hyderabad, for the award of visiting research fellowship to use the facilities at School of Chemistry, University of Hyderabad, Hyderabad and grateful to Prof. R. Chandrasekar, University of Hyderabad, for extending the lab facility. HCS is thankful to the SARCHI Research chair initiative of the Department of Science and Technology and National Research Foundation of South Africa (Grant 84415)

References

- [1] Notake, T., Takeda, M., Okada, S., Hosobata, T., Yamagata, Y. and Minamide, H. 2019. Characterization of all second-order nonlinear-optical coefficients of organic N-benzyl-2-methyl-4-nitroaniline crystal. *Scientific reports*, 9:1-8.
- [2] Khan, I. M., Ahmad, A. and Oves, M. 2010. Synthesis, characterization, spectrophotometric, structural and antimicrobial studies of the newly charge transfer complex of p-phenylenediamine with π acceptor picric acid. *Spectrochimica Acta Part A: Molecular and Biomolecular Spectroscopy*, 77:1059-1064.
- [3] Siva, G., Bharathikannan, R. and Mohanbabu, B. 2016. Growth and characterization of organic nonlinear optical material: acenaphthene DL-malic acid (ADLMA). *Journal of Optoelectronics and Advanced Materials*, 18:89-95.
- [4] Selvakumar, E., Ramasamy, P., Murugesan, V. and Chandramohan, A. 2014. Synthesis, growth and spectroscopic investigation of an organic molecular charge transfer crystal: 8-Hydroxy quinolinium 4-nitrobenzoate 4-nitrobenzoic acid. *Spectrochimica Acta Part A: Molecular and Biomolecular Spectroscopy*, 117: 259-263.
- [5] Murugesan, V., Saravanabhavan, M. and Sekar, M. 2015. Synthesis, spectroscopic characterization and structural investigation of a new charge transfer complex of 2, 6-diaminopyridine with 4-nitrophenylacetic acid: Antimicrobial, DNA binding/cleavage and antioxidant studies. *Spectrochimica Acta Part A: Molecular and Biomolecular Spectroscopy*, 147: 99-106.

- [6] Thirupugalmani, K., Venkatesh, M., Karthick, S., Maurya, K. K., Vijayan, N., Chaudhary, A. K. and Brahadeeswaran, S. 2017. Influence of polar solvents on growth of potentially NLO active organic single crystals of N-benzyl-2-methyl-4-nitroaniline and their efficiency in terahertz generation. *Crystal Engineering Communication*, 19: 2623-2631.
- [7] Vinoth, E., Vetrivel, S., Gopinath, S., Aruljothi, R., Suresh, T. and Mullai, R. U. 2019. A new class semi-organic nonlinear optical material: Mono (4-sulfo benzene aminium) tri nickel (II) bis (dihydrogen phosphate) for photonic applications. *Materials Science for Energy Technologies*, 2: 234-245.
- [8] Mohanbabu, B., Bharathikannan, R., Siva, G. 2017. Structural, optical, dielectric, mechanical and Z-scan NLO studies of charge transfer complex crystal: 3-aminopyridinium-4-hydroxy benzoate. *Journal of Materials Science: Materials in Electronics*, 28:1-10.
- [9] Evans, O. R. and Lin, W. 2002. Crystal engineering of NLO materials based on metal-organic coordination networks. *Accounts of Chemical Research*, 35:511-522.
- [10] Van der Vaart, A. and Merz Jr, K. M. 2002. Charge transfer in small hydrogen bonded clusters. *The Journal of Chemical Physics*, 116:7380-7388.
- [11] Thomas, R., Pal, S., Datta, A., Marchewka, M. K., Ratajczak, H., Pati, S. K. and Kulkarni, G. U. 2008. Charge density analysis of two proton transfer complexes: Understanding hydrogen bonding and determination of in-crystal dipole moments. *Journal of Chemical Sciences*, 120:613-620.
- [12] Babu, B., Chandrasekaran, J., Thirumurugan, R., Jayaramkrishnan, V. and Anitha, K., 2017. Experimental and theoretical investigation on 2-amino 5-bromopyridinium L-tartrate-A new organic charge-transfer crystal for optoelectronics device applications. *Journal of Materials Science: Materials in Electronics*, 28:1124-1135.
- [13] Prakash, M. J. and Radhakrishnan, T. P. 2005. SHG active salts of 4-nitrophenolate with H-bonded helical formations: Structure-directing role of ortho-aminopyridines. *Crystal Growth & Design*, 5:721-725.
- [14] Rohatgi Mukherjee, K. K. 1986. Fundamental of Photochemistry (revised ed.) *New Age International*, India, 22-25.
- [15] Miniewicz, A., Palewska, K., Sznitko, L. and Lipinski, J. 2011, Single-and Two-Photon Excited Fluorescence in Organic Nonlinear Optical Single Crystal 3-(1, 1-Dicyanoethenyl)-1-phenyl-4, 5-dihydro-1 H-pyrazole. *The Journal of Physical Chemistry A*, 115:10689-10697.
- [16] Kou, Z., Shen, J., Xu, E. and Li, S. 2013. Hybrid Coupled Cluster Methods Based on the Split Virtual Orbitals: Barrier Heights of Reactions and Spectroscopic Constants of Open-Shell Diatomic Molecules. *The Journal of Physical Chemistry C*, 117: 626-632.
- [17] Baraniraj, T. and Philominathan, P. 2009. Growth and characterization of organic nonlinear optical material: Benzilic acid. *Journal of Crystal Growth*, 311: 3849-3854.
- [18] Khan, I. M. and Ahmad, A. 2010. Synthesis, spectrophotometric, structural and thermal studies of the charge transfer complex of p-phenylenediamine, as an electron donor with π acceptor 3, 5-dinitrobenzoic acid. *Spectrochimica Acta Part A: Molecular and Biomolecular Spectroscopy*, 76:315-321.
- [19] Qiu, Y., Wang, K., Liu, Y., Deng, H., Sun, F., Cai, Y., 2007. Synthesis, characterization and 1D helical chain crystal structure of $[\text{Cu}(\text{DBA})_2(1,10\text{-phen})]_n$ and $[\text{Cd}(\text{DBA})_2(1,10\text{-phen})_2](\text{DBA}=\text{benzilic acid})$. *Inorganica Chimica Acta*, 360:1819-1824.
- [20] Ehlert, M. K., Rettig, S. J., Storr, A., Thompson, R. C., Trotter, J. and Zinc. 1990. 3,5-dimethylpyrazolate complexes: synthesis and structural studies. The crystal and molecular structure of $[\text{Zn}_2(\text{dmpz})_4(\text{Hdmpz})_2]$. *Canadian Journal of Chemistry*, 68:1494-1498.

- [21] Mohanbabu, B., Bharathikannan, R. and Siva, G. 2015. Synthesis, growth, Spectral, third order nonlinear optical and antimicrobial behaviour of 5-bromopyridine-4-hydroxybenzoic acid single crystals. *Journal of Optoelectronics and Advanced Materials*, 17:1603-1614.
- [22] Addla, D., Wen, S. Q., Gao, W. W., Maddili, S. K., Zhang, L. and Zhou, C. H. 2016. Design, synthesis, and biological evaluation of novel carbazole aminothiazoles as potential DNA-targeting antimicrobial agents. *MedChemComm*, 7:1988-1994.
- [23] Saravanabhavan, M., Sathya, K., Puranik, V. G. and Sekar, M. 2014. Synthesis, spectroscopic characterization and structural investigations of new adduct compound of carbazole with picric acid: DNA binding and antimicrobial studies. *Spectrochimica Acta Part A: Molecular and Biomolecular Spectroscopy*, 118: 399-406.
- [24] Sheldrick, G. M. 1997. SHELXS-97, Program for the solution of crystal structures, University of Gottingen, *Gottingen, Germany*.
- [25] Sheldrick, G. M. 1990. Phase annealing in SHELX-90: direct methods for larger structures. *Acta Crystallographica Section A: Foundations of Crystallography*, 46:467-473.
- [26] Cruickshank, R., Duguid, J. P., Marmion, B. P. and Awain, R. H. A. 1995. Medicinal Microbiology, 12th ed., 11, *Churchill Livingstone, London*, 196.
- [27] Collins, A. H. 1976. Microbiology Method, 2nd ed. *Butterworth, London*.
- [28] Kunchandy, E. and Rao, M. N. A. 1990. Oxygen radical scavenging activity of curcumin. *International Journal of Pharmaceutics*, 58:237-240.
- [29] Carvalho, C. C., Camargo, A. J., Tejjido, M. V., Isolani, P. C., Vicentini, G. and Zukerman-Schpector, J. 2003. Structure characterization of molecular complexes for non-linear optical materials I. X-ray analysis and AM1 calculations of 1:1 complexes of 8-hydroxyquinoline (1) and isonicotinamide (2) with 2,4,6-trinitrophenol. *Zeitschrift für Kristallographie*, 218:575-580.
- [30] Prakash, M., Geetha, D., Caroline, M. L. and Ramesh, P. S. 2011. Crystal growth, structural, optical, dielectric and thermal studies of an amino acid based organic NLO material: L-Phenylalanine L-phenylalaninium malonate. *Spectrochimica Acta Part A: Molecular and Biomolecular Spectroscopy*, 83: 461-466.
- [31] Janarthanan, S., Samuel, R. S., Selvakumar, S., Rajan, Y. C., Jayaraman, D. and Pandi, S. 2011. Growth and characterization of organic NLO crystal: β -naphthol. *Journal of Materials Science & Technology*, 27: 271-274.
- [32] Willard, H., Merritt, L. L., Dean, J. A. and Settle, F. A. 1986. Instrumental Methods of Analysis, Wadsworth publishing company, USA.
- [33] Hameed, A. H., Ravi, G., Dhanasekaran, R. and Ramasamy, P. 2000. Studies on organic indole-3-aldehyde single crystals. *Journal of Crystal Growth*, 212: 227-232.
- [34] Bamzai, K. K., Kotru, P. N. and Wanklyn, B. M. 1998. Investigations on indentation induced hardness and fracture mechanism in flux grown DyAlO₃ crystals. *Applied Surface Science*, 133: 195-204.
- [35] Onitsch, E. M. 1947. Über die mikrohärtete der metalle. *Microscopia*, 2:131.
- [36] Hanneman, M. and Metall. 1941. *Manch*, 23:135-140.
- [37] Wooster, W. A. 1953. Physical properties and atomic arrangements in crystals. *Reports on Progress in Physics*, 16: 62.
- [38] Kowski, P. W., Kantorow, S. B., Mączka, D. and Stelmakh, V. F. 1989. Processes of Radiation Defect Interaction and Amorphisation of Silicon at Large Implantation Doses. *Physica Status Solidi (a)*, 112: 695-698.
- [39] Balarew, C. and Duhlev, R. 1984. Application of the hard and soft acids and bases concept to explain ligand coordination in double salt structures. *Journal of Solid State Chemistry*, 55: 1-6.

- [40] Sheik-Bahae, M., Said, A. A. and Van Stryland, E. W. 1989. High-sensitivity, single-beam n_2 measurements. *Optics Letters*, 14: 955-957.
- [41] Sheik-Bahae, M., Said, A. A., Wei, T. H., Hagan, D. J. and Van Stryland, E. W. 1990. Sensitive measurement of optical nonlinearities using a single beam. *IEEE Xplore: IEEE Journal of Quantum Electronics*, 26: 760-769.
- [42] Gomez, S. L., Cuppo, F. L. S. and FigueiredoNeto, A. M. 2003. Nonlinear optical properties of liquid crystals probed by Z-scan technique. *Brazilian Journal of Physics*, 33: 813-820.
- [43] Sheik-Bahae, M., Hutchings, D. C., Hagan, D. J. and Van Stryland, E. W. 1991. Dispersion of bound electron nonlinear refraction in solids. *IEEE Xplore: IEEE Journal of Quantum Electronics*, 27: 1296-1309.
- [44] Rosenberg, B., Van Camp, L. and Krigas, T. 1965. Inhibition of cell division in *Escherichia coli* by electrolysis products from a platinum electrode. *Nature*, 205: 698-699.
- [45] Wolfe, A., Shimer Jr, G. H. and Meehan, T. 1987. Polycyclic aromatic hydrocarbons physically intercalate into duplex regions of denatured DNA. *Biochemistry*, 26: 6392-6396.
- [46] Nafisi, S., Saboury, A. A., Keramat, N., Neault, J. F. and Tajmir-Riahi, H. A. 2007. Stability and structural features of DNA intercalation with ethidium bromide, acridine orange and methylene blue. *Journal of Molecular Structure*, 827: 35-43.
- [47] Cruickshank, R., Duguid, J. P., Marmion, B. P. and Awain, R. H. A. 1995. *Medicinal Microbiology*, 12, 11, Churchill Livingstone, London, 196.